Proceedings of the 26th Annual International Conference of the IEEE EMBS
San Francisco, CA, USA • September 1-5, 2004

Stochastic modeling and validation of growth saturation and radiotherapeutic response of multicellular tumor spheroids

E. I. Zacharaki, G. S. Stamatakos, K. S. Nikita and N. K. Uzunoglu
School of Electrical and Computer Engineering, National Technical University of Athens, Athens, Greece

Abstract—**An advanced three-dimensional (3D) Monte Carlo simulation model of both the avascular development of multicellular tumor spheroids and their response to radiation therapy is presented. The model is based upon a number of fundamental biological principles such as the transition between the cell cycle phases, the diffusion of oxygen and nutrients and the cell survival probabilities following irradiation. Predicted histological structure and tumor growth rates evaluated for the case of EMT6/Ro spheroids have been shown to be in agreement with published experimental data. Furthermore, the underlying structure of the tumor spheroid as well as its response to irradiation satisfactorily agrees with laboratory experience.**

Keywords— **fractionation, multicellular spheroid, radiation, radiosensitivity, simulation model, tumor growth**

I. Introduction

Tumor growth computer simulation models aim at three-dimensionally predicting and visualizing both the growth and the response of tumors to therapeutic schemes with respect to time. Such a model can provide an efficient platform for gaining insight into the (radio)biological mechanisms involved in tumor growth *in vitro* as well as during the avascular stages of *in vivo* tumor evolution. Optimization of dose fractionation during radiation therapy by performing *in silico* experiments before the actual delivery of the radiation dose to the patient is the main practical target. A further application might be the partial replacement of current expensive (in terms of both time and money) *in vitro* oncologic experiments by computer simulations.

The proposed approach is based on a discrete time cell cycle model, which is applied to each one of the cells constituting the tumor. The discrete time and space character of such a model allows the imposition of arbitrary boundary conditions such as the spatial profile of the oxygen and glucose supply. Therefore, this kind of model can be easily extended to the *in vivo* case [1], where the presence of different tissues producing variable elastic and nutrient supply profiles in the vicinity of a tumor can greatly affect the growth pattern. Moreover, all apparently possible pathways in the cellular level leading to cell death have been incorporated including interphase cell death via either spontaneous or radiation induced apoptosis, as well as mitotic cell death through either necrosis or apoptosis.

Special emphasis is placed on the adjustment of the model output to experimental data. To this end, some previous model assumptions [1] have been modified in order to refine the description of the involved phenomena.

II. Methodology

The model formulation is based on the cellular level. Angiogenesis is not taken into account. This is a plausible hypothesis for both tumor growth in cell culture and the non-vascularized tumor or metastatic nodule growth *in vivo*. The statistical character of specific biological phenomena during cell proliferation and irradiation is simulated applying a pseudo-random number generator. In the following, the model assumptions are briefly described [1]-[3].

A. Tumor growth kinetics

1) A tumor cell, when cycling, passes through the phases G_1 (gap 1), S (DNA synthesis), G_2 (gap 2) and M (mitosis). The durations of the various cell states follow normal (Gaussian) distribution. After mitosis is completed, each one of the resultant cells re-enters G_1 if oxygen and nutrient supply in its current position is adequate. Otherwise, it enters the resting G_0 phase.

2) A cell stays in the G_0 phase for as long as its distance (r) to glucose and oxygen supply is greater than the thickness of the proliferating cell layer (W_P) and lower than the thickness of the viable cell layer (W) (Fig. 1). If the local environment of the cell becomes adequate ($r<W_P$) the cell re-enters G_1. Conversely a cell, deprived of oxygen or glucose ($r>W$), looses its energy-producing capacity and enters necrosis (N) [4].

3) The thickness of the viable rim decreases linearly as a function of the spheroid diameter [4]-[6]. As the proliferating cell rim is part of the viable rim, the same decrease rate has been assumed. The thickness of the hypoxic cell rim (W_{G0}) can be calculated as the difference of the viable and the proliferating cell rim.

4) In addition to the previously described pathway, there is always a probability that each cell residing in any phase (other than necrosis or apoptosis) dies with some probability per hour due to both ageing and spontaneous apoptosis (A). This probability representing the cell loss rate due to apoptosis (*CLRA*) is the product of the cell loss factor due to apoptosis (with a typical value of e.g. 10%) and the cell birth rate [7]. The cell birth rate can be considered as the ratio of the growth fraction (with a typical value of e.g. 40%) [7] to the cell cycle duration.

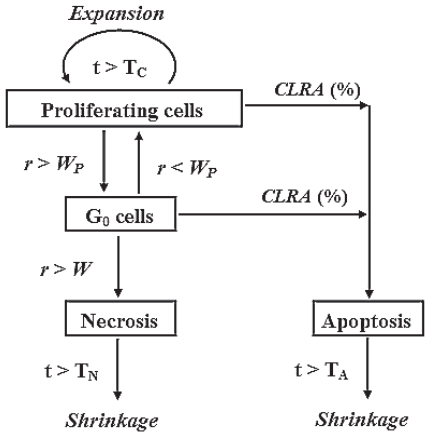

Fig. 1. Schematic representation of the transition between the various cell phases during pure growth according to temporal (t) and spatial (r) model parameters. T_C: cell cycle duration, T_N: duration of necrosis, T_A: duration of apoptosis.

B. Tumor Geometry

1) A 3D mesh discretizing the volume occupied by the cell culture is used. This volume includes the tumor as well as part of the surrounding nutrient medium. Each cubic geometrical cell of the mesh can be occupied by a viable tumor cell (Fig. 3), by products of cell death (either necrotic or apoptotic) or by the nutrient medium. The total space occupied by the simulated cell culture has been confined to $120\times120\times120$ mesh cells. This limit depends on the available computer memory and power as well as on the maximum tolerable runtime.

2) The discretizing mesh consists of cubic geometrical cells, each one including a single tumor cell as well as the corresponding intracellular medium. The tumor spheroid diameter (D) is calculated according to the equation

$$D = 2\sqrt[3]{\frac{3}{4\pi}N\cdot d_C{}^3}\ , \qquad (1)$$

where d_c is tumor cell diameter and N is the number of the geometrical cells occupied by the tumor spheroid [2].

3) Communication between cells at any angular direction is possible. Tumor shrinkage and tumor expansion is computationally achieved by shifting a cell chain according to appropriate algorithms [2].

C. Tumor Cell Response to Irradiation

1) The response of each cell to irradiation, leading to absorbed dose d is described by the LQ model [8]. According to this model, the survival probability $S(d)$ of the cell is given by the expression

$$S(d) = \exp\left[-\left(\alpha d + \beta d^2\right)\right], \qquad (2)$$

where α and β are parameters describing the radiobiological properties of the specific tumor [7]. It is noted that (2) is effective after the expiration of a time interval sufficient for the sublethal damage to be repaired (i.e. 4 h after irradiation).

2) Cells in any cell cycle phase are more radiosensitive than hypoxic cells residing in G_0, which is simulated by assuming different sets of values for the α and β parameters of the LQ model [8]: (α_P, β_P) for the proliferating cells except the cells in the S phase and (α_{G0}, β_{G0}) for the dormant cells. The radiobiological parameters α_S and β_S for the cells in the S phase have been assumed smaller than the α_P and β_P values because cells in the S phase are more radioresistant than cells in any other cycle phase (G_1, G_2 and M). Moreover, α_S and β_S values have been assumed closer to the values of the radiobiological parameters of the rest of the proliferating cells than to those of the dormant cells ($\alpha_S = 0.7\,a_P + 0.3\,a_{G0}$, $\beta_S = 0.7\beta_P + 0.3\beta_{G0}$).

3) The radiation dose under hypoxia producing the same level of biological effect as the dose under aerobic conditions is equal to the latter multiplied by a factor, called the oxygen enhancement ratio (*OER*) [7]. This observation can be formulated according to (2) as

$$\exp\left[-\left(\alpha_{G0}OER\cdot d + \beta_{G0}\left(OER\cdot d\right)^2\right)\right] = \exp\left[-\left(\alpha_P d + \beta_P d^2\right)\right] \qquad (3)$$

and can be satisfied if

$$a_{G0} = \frac{a_P}{OER} \text{ and } \beta_{G0} = \frac{\beta_P}{OER^2} \qquad (4)$$

The *OER* value for X-rays is around 3.0 for most cells [7].

4) The cell death due to irradiation is simulated by three mechanisms: the radiation induced interphase death, the radiation induced mitotic necrotic death and the radiation induced mitotic apoptotic death [9]. Each irradiated cell residing in the G_0 phase that will not survive according to the LQ model can die by either apoptosis (with a 20% probability) or necrosis (with an 80% probability). Cycling cells being exposed to ionizing radiation can die either before entering division through apoptosis (interphase death, with a 20% probability) or after having completed several divisions (e.g. 3) either through apoptosis (mitotic apoptotic death, 10% probability) or through necrosis (mitotic necrotic death, 70% probability). The probability of occurrence of mitotic death has been assumed much higher than the probability of interphase death, since for the most cell lines *in vitro* the primary form of cell death is associated with mitosis [9].

III. RESULTS

As EMT6 (mammary sarcoma of the mouse) spheroids are very often and effectively used in therapy-related experimentation, the developed model has been applied to this specific case. As a typical (mean) cell volume in an EMT6/Ro spheroid is 2500 μm^3 [10], the mean cell diameter has been calculated to be d_c = 16.8μm. The thickness W of the viable cell layer tends to behave as a linear function of the spheroid diameter D. The slope of the thickness depends on the glucose concentration and typically varies between –

0.017 and –0.052 in the case of EMT6/Ro spheroids [4]. The corresponding equation is

$$W(D) = -0.025D + W_0, \quad (5)$$

where W_0 is a constant depending on the spheroid diameter at which necrosis first develops. The onset of necrosis depends on the nutrient concentration. Under normal conditions (0.28 mM oxygen and 5.5 mM glucose concentration) necrosis initially develops at a diameter of ~400 μm, resulting in $W_0 = 210$ μm. The thickness of the proliferating cell layer has been assumed to be $W_P(D) = -0.025D + W_{P0}$. According to [10],[11] the spheroid diameter at which hypoxia first develops is ~300 μm in EMT6/Ro spheroids. In the same way W_{P0} is calculated ($W_{P0} = 157.5$ μm).

Typical mean values and standard deviations of the phase durations of the constituting cells for the EMT6 spheroid are shown in [2],[11].

A. Growth

Fig. 2a shows the total number of viable cells of a multicellular tumor spheroid of a mammary sarcoma of the mouse grown in cell culture as a function of the growth time redrawn from Freyer *et al.* [10] with permission. Fig. 2b shows the prediction of the suggested simulation model of the volumetric growth representing the mean values of 3 simulation runs each one having different seed of the random number generator. The Gompertzian pattern of tumor growth is explained by the absence of blood vessels in cell cultures. The cell cycle duration and the time required for cell death and tumor shrinkage determine the temporal evolution of the spheroid. As expected, the volume growth becomes saturated over time. The mechanism simulating the spheroid saturation can be described as a modulation of the spheroid size. If W_P were constant, i.e. independent of the spheroid diameter, the tumor growth rate would decrease with time as the percentage of the proliferating cells is decreasing. In such a case, although the initial stages of the Gompertzian growth are satisfactorily simulated, the growth saturation stage tends to be poorly predicted [1],[3].

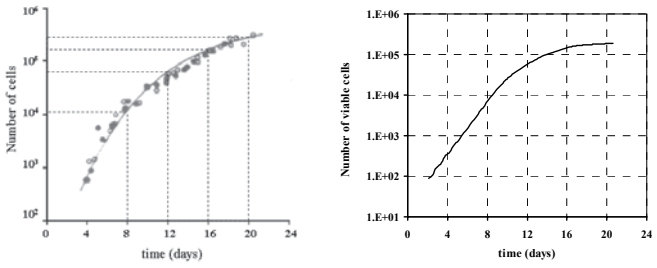

(a) Experimental data (b) Simulation predictions

Fig. 2. Growth of a multicellular EMT6/Ro tumour spheroid as a function of time: (a) experimental as appeared in Freyer *et al.* (with permission) [10] and (b) simulated.

TABLE I
EXTENT OF CENTRAL NECROSIS AS A FUNCTION OF THE SPHEROID DIAMETER

D (μm)	468	821	1156	1347
Experimental (%)	>1	12	28	38
Simulated* (%)	0.4	18	32	39

* (Necrotic Volume / Total Volume) ×100%. The apoptotic products constituting approximately 1.2% of the total tumour volume have not been taken into account.

Table I presents the portion of central necrosis in the total tumor volume as a function of the spheroid diameter. The simulation data have been compared with experimental data derived by Freyer *et al.* [10]. The diameter of the simulated tumor spheroid at the onset of necrosis has been shown to be practically the same as the experimental one (400 μm). The central necrosis depends mostly on the viable and the proliferating rim thickness (onset and slope value) as well as on the time duration of necrosis.

Fig. 3 has been produced using the visualization package AVS/Express 4.2. and depicts a 3D representation of the internal structure of an EMT6 tumor spheroid. The snapshot corresponds to the instant 400 h after the placement of a single tumor cell in the phase of mitosis at the center of the discretizing mesh.

B. Simulation of Fractionated Radiotherapeutic Schemes

Simulations of the application of different fractionated schemes on a heterogeneous spheroid population offer a further tool for the extrapolation of the results to the *in vivo* case of solid avascular tumors. Therefore, an EMT6 spheroid of diameter ~1500 μm where hypoxia is present has been virtually (*in silico*) irradiated according to five common fractionated radiotherapeutic schemes [2]. Estimates for the values of the α_P and β_P parameters of the radiobiological LQ model have been derived from [11] ($\alpha_P = 0.21$, $\beta_P = 0.028$). The model has proved to be able to effectively simulate the rather periodical tumor cell number decrease caused by the dose fractions, as well as the repopulation effect of the weekend pause.

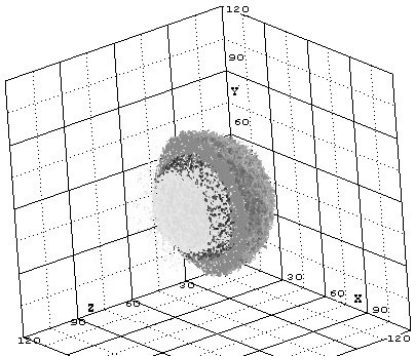

Fig. 3. A 3D representation of the internal structure of an EMT6 tumor spheroid using AVS/Express™ 4.2 The proliferating (gray) and hypoxic cell rim (black) enclose the necrotic core (light gray).

The tumor response to irradiation is strictly dependent on the duration of the cell cycle and the α and β values. The latter has been demonstrated by performing a parametric analysis of the response to a specific radiation therapy scheme for different radiobiological values. For this purpose, the standard fractionation scheme has been chosen: 2 Gy once a day, 5 days a week, 60 Gy in total, 6 hours time interval between fractions. Fig. 4 displays the temporal response of the same tumor spheroid for the values α_P in the range 0.2 - 0.6 Gy^{-1} and $\beta_P = 0.1\,\alpha_P$ each time. The corresponding values α_S, β_S, α_{G0}, β_{G0} are calculated as previously described. The curves shown in Fig. 4 demonstrate that the model is sensitive to a decrease of tumor radioresistance. The curve corresponding to $\alpha_P = 0.2$ Gy^{-1} is most relevant to an EMT6 tumor [11].

IV. Discussion

The proposed simulation model has been based on discrete spatiotemporal rules describing the (radio)biological behavior of a 3D tumor spheroid instead of applying complex mathematical formulations. The model has been applied to the specific case of EMT6 tumor spheroids. Nevertheless, it can simulate the basic growth pattern characteristics that have been established for spheroids of many other cell types and cell lines, i.e. volume growth saturation, development of an outer proliferating rim and a growing necrotic center. Apart from the provision of the cytokinetic and radiobiological data for the specific tumor cells, no modifications to the code are in principle necessary. Obviously, experimental feedback should always be used in order to improve the reliability of the model.

A typical simulation run of 5 weeks for 120×120×120 geometrical cells takes about 5 min on an AMD Athlon XP 1800 machine (786MB RAM). The Visual Fortran 6.0 programming language has been used.

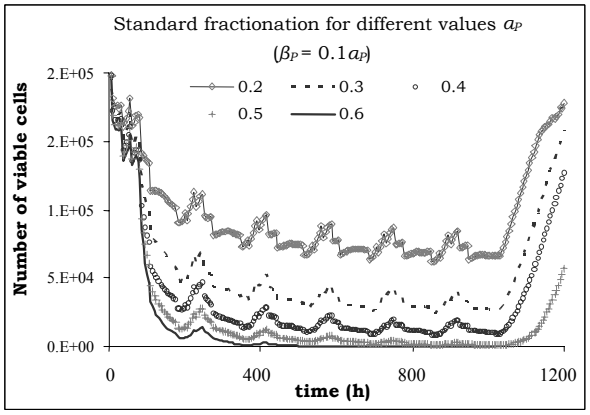

Fig. 4. Number of viable cells as a function of time for different radiobiological values. The standard fractionation scheme is applied.

V. Conclusion

The goal of this paper was to provide both the basic scientist and the clinician with an advanced computational tool for gaining insight into the biology of tumor behavior and supporting the process of biological optimization of radiation therapy. The tumor structure (including the well oxygenated, the hypoxic and the necrotic layers) was adapted to the experimental situation of EMT6/Ro tumor spheroids by exploiting published physiological data concerning oxygen, nutrient and cell death product diffusion. The excellent agreement of the model predicted with the experimentally observed growth rate and extent of central necrosis supports the validity of the model.

References

[1] G.S. Stamatakos, D.D. Dionysiou, E.I. Zacharaki, N. Mouravliansky, K.S. Nikita and N.K. Uzunoglu, "In Silico Radiation Oncology: Combining Novel Simulation Algorithms with Current Visualization Techniques," *Proceedings of the IEEE*, vol. 90, pp. 1764–1777, 2002.

[2] E.I. Zacharaki, G.S. Stamatakos, K.S. Nikita and N.K. Uzunoglu, "Simulating growth dynamics and radiation response of avascular tumour spheroids – Model validation in the case of an EMT6/Ro multicellular spheroid," *Computer Methods and Programs in Biomedicine*, in press.

[3] G.S. Stamatakos, E.I. Zacharaki, M. Makropoulou, N. Mouravliansky, A. Marsh, K.S. Nikita, and N.K. Uzunoglu, "Modeling tumor growth and irradiation response in vitro- a combination of high-performance computing and web based technologies including VRML visualization," *IEEE Trans. Inform. Technology Biomedicine*, vol.5, pp. 279–289, 2001.

[4] J.P. Freyer and R.M. Sutherland, "Regulation of growth saturation and development of necrosis in EMT6/Ro multicellular spheroids by the glucose and oxygen supply," *Cancer Research*, vol. 46, pp. 3504–3512, 1986.

[5] A.C. Burton, "Rate of growth of solid tumours as a problem of diffusion," *Growth*, vol. 30, pp. 157-176, 1966.

[6] J. Landry, J.P. Freyer, and R.M. Sutherland, "A model for the growth of multicell tumour spheroids," *Cell Tissue Kinet*., vol.15, pp. 585–594, 1982.

[7] G. Steel, *Basic Clinical Radiobiology*, London, UK: Arnold, 1997, pp. 15, 47–48, 52–57, 123–133, 153, 161

[8] A.J. Mundt, J.C. Roeske, R.R. Weichselbaum, "Physical and Biologic Basis of Radiation Oncology," in *Cancer Medicine*, 5th edition, R.C. Bast, D.W. Kufe, R.E. Pollock, R.R. Weichelbaum, J.F. Holland, E. Frei, Eds. Canada: BC Decker Inc, 2000.

[9] W.C. Dewey, C.C. Ling, R.E. Meyn, "Radiation-induced apoptosis: relevance to radiotherapy," *Int. J. Radiation Oncology Biol. Phys.*, vol. 33, pp. 781–796, 1995.

[10] J.P. Freyer, R.M. Sutherland, "A reduction in the in situ rates of oxygen and glucose consumption of cells in EMT6/Ro spheroids during growth," *Journal of Cellular Physiology*, vol. 124, 516–524, 1985.

[11] T. Ginsberg, *Modellierung und Simulation der Proliferationsregulation und Strahlentherapie normaler und maligner Gewebe*, Reihe 17: Biotechnik, Nr 140, Duesseldorf: Fortschritt-Berichte, VDI Verlag, 1996, pp.103–107.